Chemosphere 335 (2023) 139092

Contents lists available at ScienceDirect

Chemosphere

journal homepage: www.elsevier.com/locate/chemosphere

Alginate/geopolymer hybrid beads as an innovative adsorbent applied to the removal of 5-fluorouracil from contaminated environmental water

Assia Ben Amor [a,b], Marina Arenas [c], Julia Martín [c,*], Abdelkader Ouakouak [d,e], Juan Luis Santos [c], Irene Aparicio [c], Esteban Alonso [c], Noureddine Hamdi [a,b]

[a] Higher Institute of Water Sciences and Techniques, University of Gabès, Zrig 6072, Tunisia
[b] Laboratoire des Matériaux Composites et Matériaux Argileux, CNRSM, Technopole Borj Cedria B.P. 73, 8027, Soliman, Tunisia
[c] Departamento de Química Analítica, Escuela Politécnica Superior, Universidad de Sevilla. E-41011 Seville, Spain
[d] Research Laboratory in Subterranean and Surface Hydraulics, University of Biskra, PO Box 145 RP, Biskra, 07000, Algeria
[e] Hydraulic and Civil Engineering Department, University of El Oued, PO Box 789, El Oued, 39000, Algeria

HIGHLIGHTS

- Alginate/geopolymer hybrid beads were synthetized using extrusion method.
- >80% of 5-FU in a 2.5 mg/L solution was removed with a dosage of 0.02 g AGHB/10 mL.
- The adsorption equilibrium was reached very fast (<60 min).
- 5-FU adsorption onto AGHB is well described by the Langmuir model and PSO model.
- High potential of AGHB to be used in environmental contaminated water.

GRAPHICAL ABSTRACT

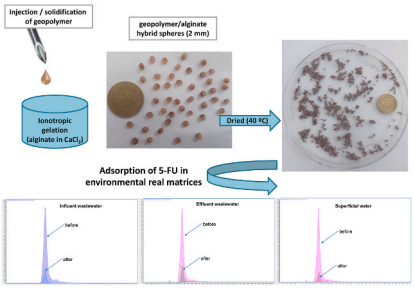

ARTICLE INFO

Handling Editor: Xiangru Zhang

Keywords:
Biocomposite
Hybrid material
Cytostatic drugs
Adsorption
Environmental water

ABSTRACT

Water contaminated by cytostatic drugs has many negative impacts on the ecosystems. In this work, cross-linked adsorbent beads based on alginate and a geopolymer (prepared from an illito-kaolinitic clay) were developed for a promising decontamination of the 5-fluorouracil (5-FU) cytostatic drug from water samples. The characterization of the prepared geopolymer and its hybrid derivative was performed by scanning electron microscopy, X-ray diffraction, Fourier transform infrared and termogravimetric analysis.

Batch adsorption experiments indicated that alginate/geopolymer hybrid beads (AGHB) allow an excellent 5-FU removal efficiency of up to 80% for a dosage adsorbent/water of 0.002 g/mL and a concentration of 5-FU of 2.5 mg/L. The adsorption isotherms data follow well the Langmuir model. The kinetics data favor the pseudo-second-order model. The maximum adsorption capacity (q_{max}) was 6.2 mg/g. The optimal adsorption pH was 4. Besides pore filling sorption process, the carboxyl and hydroxyl groups from alginate immobilized onto the geopolymer matrix favored the retention of 5-FU ions by hydrogen bonds. Common competitors, such as dissolved organic matter, do not significantly affected the adsorption. In addition, this material has not only eco-friendly and cost-effective advantages but also excellent efficiency when applied to real environmental

* Corresponding author.Julia Martín Departamento de Química Analítica Escuela Politécnica Superior Universidad de Sevilla c/ Virgen de África, 7 41011, Seville, Spain.
E-mail address: jbueno@us.es (J. Martín).

https://doi.org/10.1016/j.chemosphere.2023.139092
Received 6 March 2023; Received in revised form 27 May 2023; Accepted 30 May 2023
Available online 31 May 2023

samples such as wastewater and surface water. This fact suggests that it could have a great application in the purification of contaminated water.

1. Introduction

Cytostatic drugs are compounds extensively used in chemotherapy for cancer treatment (Heath et al., 2020). Since 1957, 5-Fluorouracil (5-FU) has been widely prescribed as an antineoplastic agent to treat many types of cancers such as breast, colon, head, neck ~~or~~ and pancreatic endocrine cancers (Kosjek et al., 2013). Human excreta of this drug after administration contributes to its release ~~in~~to wastewater, and, in such way, to enter into the environment affecting mainly the aquatic ecosystems (de Oliveira Klein et al., 2021; Misík et al., 2019; Heath et al., 2020). Concentration levels of 5-FU up to 122 μg/L, 280 ng/L and 160 ng/L have been reported in hospital effluents, effluent wastewaters and superficial waters, respectively (Heath et al., 2020; Booker et al., 2014). Its pharmacological activity, along with its genotoxic, cytotoxic, mutagenic, and teratogenic properties, potentially makes 5-FU one of the most dangerous contaminants in the aquatic ecosystems (Orias and Perrodin, 2014; Heath et al., 2020).

A low elimination rate of 5-FU using traditional physicochemical (flocculation, filtration, and coagulation) (Wilczewska et al., 2022; Kulaksız et al., 2022) and biological (Dinesh and Chakma, 2019; Zhang et al., 2017) wastewater treatments has been reported in several studies. The simplicity of adsorption, low start-up costs, environmentally friendly alternatives and wide availability of adsorbents make this technique an effective alternative to treat contaminated water (Kulaksiz et al., 2022; Hacıosmanoglu et al., 2022; Orta et al., 2020; Martín et al., 2019; Luhar and Luhar, 2021; Yahyavi et al., 2020).

Geopolymer technology is receiving increasing interest in the industrial and household waste field. Geopolymers constitute a versatile material to be used as adsorbents. They are synthetized by a reaction between an aluminosilicate (also power plant by-products) and a highly alkaline solution, at low temperature. The resulted material exhibits a 3D network amorphous or semicrystalline structure with a high physicochemical stability and porous and high specific surface area (Davidovits, 2008). Additionally, to increase its range of applications, the geopolymer matrix can be tailored with its particular functionality (Ge et al., 2017; Li et al., 2015). In this sense, the combination of the biodegradability properties of biopolymers, together with the compatibility of geopolymers with other materials, is a successful way to develop selective composites that can be used for environmental remediation. Biopolymeric resins have an expandable surface and enhanced compatibility with organic pollutants and higher regeneration capacity. Polysaccharides, such as chitosan or alginate, are excellent options owing to their low-cost and non-toxic properties. Different dripping techniques, such as injection and solidification methods, in polyethylene glycol, liquid N_2, or ionotropic gelation (alginate in $CaCl_2$) have been proposed to produce hybrid beads of these two different materials (Ge et al., 2017; Medri et al., 2020). Compared to traditional powder adsorbent, it has been reported that beads can increase the adsorption capacity, as they present a larger surface area and better mass transfer and diffusion behavior (Ge et al., 2017; Li et al., 2015).

Alginate is a natural polysaccharide comprising abundant hydroxyl and carboxyl moieties. Adsorbents synthesized from sodium alginate exhibit large uptake capacities of ions and organic molecules through electrostatic interactions, hydrogen bonds and chemical bonds (Ucankus et al., 2018). However, their industrial applications are limited because of their poor physical strength and thermostability. Thus, the combination with geopolymers is an interesting alternative to be used in water purification. To the date, alginate/geopolymer composites have been developed and proposed for removing heavy metals or methylene blue as model compounds. Papa et al. (2021) prepared hybrid beads combining a metakaolin-based geopolymer with alginate and hydrotalcite powder. Ge et al. (2017) synthetized hybrid beads from metakaolin geopolymer and sodium alginate. Their results suggested that this material exhibits a high removal efficiency for copper ions. However, to our knowledge, the effect of the geopolymer modification on the adsorption capacity of pharmaceuticals from contaminated water has been scarcely investigated to the date (Al-husseiny and Ebrahim, 2021; Luhar and Luhar, 2021; Abukhadra et al., 2022).

The present study involved the synthesis and characterization of a novel adsorbent. The synthesis was carried out using a simple method by incorporating porous geopolymer (an inorganic illito-kaolinitic clay) and sodium alginate (organic) and crosslinking alginate and calcium ions, to combine their special properties. Once synthetized, the applicability of the novel material to the decontamination of 5-FU from water samples was tested. The adsorption batch studies were carried out at different concentrations of 5-FU, contact time, and environmental conditions (pH and dissolved organic matter (DOM)). The applicability of the novel material in the removal of 5-FU was finally tested in real environmental water samples.

2. Experimental work

2.1. Standards and reagents

Pure 5-FU (>99%), analytical-grade reactive calcium chloride, sodium hydroxide, ~~and~~ hydrochloric acid and formic acid were purchased from Sigma Aldrich. Sodium alginate was obtained from Biochem Chemopharma Laboratory Reagent. HPLC-grade water and acetonitrile were supplied by Romil (Barcelona, Spain).

All solutions were prepared using deionized water.

Aluminosilicate minerals used to prepare the geopolymer were extracted from an illito-kaolinitic clay from Douriet region in South-East of Tunisia. They were taken from sedimentary Aptian materials (chemical composition is detailed in Table S1). The waste glass powder was obtained by grinding the waste glass and sieving it to a particle size of 150 mm. The commercial silica fume powder was supplied by Iran Ferroalloy Industries Company (chemical composition is detailed in Table S1).

2.2. Methods

2.2.1. Preparation of geopolymer

The precursors used to prepare the geopolymer are described in Table S2. The procedure is schematized in Fig. S1. First, the Douiret clay was crushed and ground using a ball mill and then sieved through 150 mm. The material was then calcined at 750 °C for 2 h to obtain, by dihydroxylation, metekolin (Douiret calcined).

The Douriet calcined clay powders were mixed with NaOH solution (12 M) for 15 min. Then, the glass waste powders were added to the mixture until dissolution. The silica fume powders were mixed with NaOH solution until dissolution. The paste samples were cast in cylindrical PVC molds (20 mm of diameter and 40 mm of height) and were vibrated for 5 min to eliminate trapped air bubbles. The curing stage for the preparation of geopolymers was carried out in a conventional oven at 70 °C in an open mold. Fig. S2 shows a picture of the geopolymer specimen.

2.2.2. Preparation of alginate/geopolymer hybrid bead composite

The AGHB were synthetized applying the extrusion method by mixing alginate/geopolymer using a syringe in a solution containing a cross-linking agent. The geopolymer was powdered using a ball mill. An amount of 2 g of geopolymer was mixed with a sodium alginate solution

(2.0 wt%) under stirring for 1 h. Then, the mixture was dropped through a syringe into a calcium chloride solution (4 wt%) to form the hybrid beads. The beads were dried at 40 °C. The obtained product is shown in Fig. 1.

The crosslinking between Ca^{2+} and alginate became much stronger at high amounts of sodium alginate. However, an excess of sodium alginate results in an excessive solidification what can block the inner pores of geopolymer matrix. Because of that, sodium alginate solution concentration was set at 2% wt% according to experiments from Ge et al. (2017) and Aichour and Zaghouane-Boudiaf (2020).

2.3. Characterization analysis

The microstructural features of the geopolymer and its derivative AGHB were studied by a scanning electron microscope (FEI-TENEO). Previously, samples were made conductive by applying a thin gold layer using a turbo-pumped sputter coater. The specific area and porosity of the samples were measured by the Brunauer–Emmett–Teller (BET) technique. Adsorption/desorption isotherms were obtained using an accelerated surface area and a porosimetry system (ASAP 2420). The Barret-Joyner-Halenda (BJH) method was used for the quantification of the pore volume. The diameter size distribution in the range of 0.020–2000 μm was analyzed by a Mastersizer 2000 equipment (Malvern instruments). The XRD pattern of the geopolymer and its derivative AGHB was examined using a Bruker D8 Advance A25 diffractometer (Bruker, Germany). Functional groups were observed by Fourier transform infrared spectrometry (FTIR) using a Cary 630 FTIR (Agilent, USA) with diamond attenuated total reflection. The charge of the material was measured using a Zetasizer Nanosystem system (Malvern Instruments, Southborough, MA). The pH of the zero-point charge (pH_{ZPC}) was determined by the pH drift method using a BASIC 20 pH-meter (Crison Instruments, Barcelona, Spain).

2.4. Batch adsorption assays

Batch adsorption assays of 5-FU onto AGHB were carried out by mixing 20 mg of AGHB with 10 mL aqueous solutions at different concentrations of 5-FU, contact time, and environmental conditions (pH and DOM). At the end of each experiment, the solutions were filtrated through 0.22 μm filters. All experiments were carried out in triplicate. The procedural blanks, without AGHB, were simultaneously processed.

The residual 5-FU concentrations were quantified using liquid chromatography coupled with tandem mass spectrometry (Agilent, Santa Clara, CA, USA). 5-FU was isolated using a HALO C-18 Rapid Resolution column (50 × 4.6 mm id, 2.7 μm) and a mobile phase composed of ammonium acetate (10 mM) (solvent A) and methanol (solvent B). The mass spectrometer was operated in negative electrospray ionization mode. $[M - H]^-$ was used as precursor ion (m/z 129). The analyses were performed in multiple reaction monitoring mode using the transition m/z 129 => 42.1 for quantification purposes.

The adsorption amount (q_e) (mg/g) and removal efficiency (%)were calculated as follows:

$$q_e = V\cdot(C_0–C_e)/m$$

$$R=(C_0–C_e)/C_0\cdot 100$$

where C_0 and C_e (mg/L) are the initial and equilibrium concentrations of 5-FU in the water solution, respectively; V is the volume of the water solution (0.01 L in all cases); and m is the AGHB dosage (0.02 g in all cases). Kinetic and isotherm models applied to the obtained data are described in the supplementary material.

3. Results and discussion

3.1. Characterization

3.1.1. Characterization of raw materials based geopolymers

Table S1 shows chemical analysis applied to the raw materials used to prepare the geopolymer. The composition of the original illito-kaolinitic Douriet clay is represented by the main oxides including SiO_2, Al_2O_3, Fe_2O_3, K_2O, MgO and Na_2O, whereas CaO, SO_3 and TiO_2 are present at trace amounts. The sample contains a relatively high quantity of potassium (average: 4.41%) and alkalis (K_2O + Na_2O) (average: 5.34%). The material presents three main fractions: (1) clay fraction (<2 μm), which represents approximately 10%; (2) silt fraction, known for its particle size ranging between 2 and 20 μm (55% of the Douiret clay); (3) and the remaining coarse fraction with a particle size higher than 20 μm (35%).

The glass waste contains large amounts of silica with 71.44% by mass.

The mineralogical changes during the firing process were analyzed by XRD. The X-ray diffractograms of the raw clays after heating at 750 °C for 2 h are given in Fig. S3. Kaolinite, present in Douiret clay disappears completely in the calcined material at 750 °C. Illite, on the other hand, gradually decreased at a temperature of 750 °C. Dolomite minerals underwent the same process as illite. Quartz was the only mineral that resisted.

The FTIR spectrum of the raw material (Fig. S4) shows the presence of Al–OH as stretching bands at 3612-3683 cm^{-1} and as bending bands at 920 cm^{-1}. Moreover, a bending band at 690 cm^{-1} characterizes the

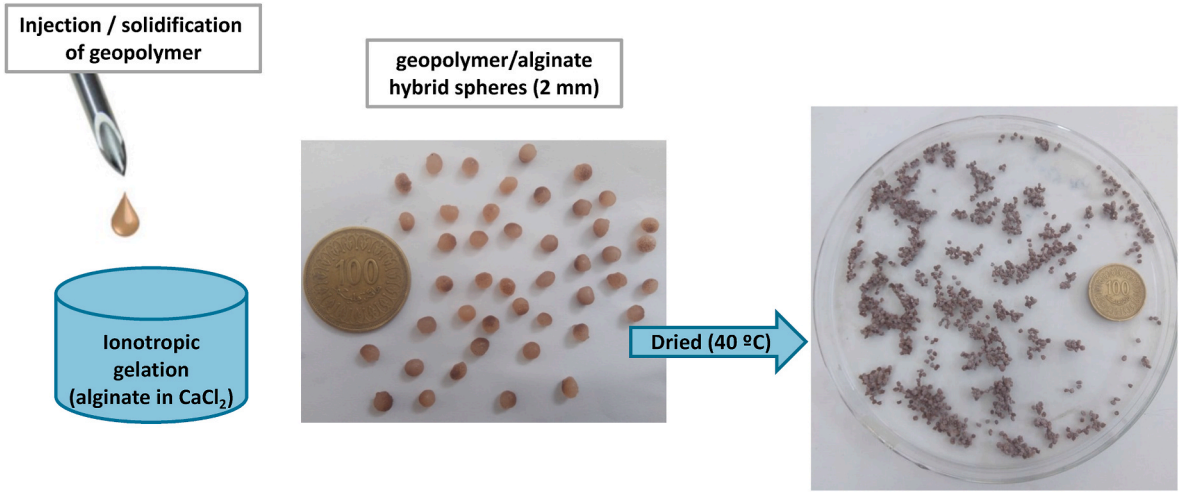

Fig. 1. Schematic diagram of the production process of AGHB by extrusion method.

kaolinite mineral (Caillère et al., 1982). It is quite difficult to identify illite especially by infrared techniques. The main mineral impurity was quartz. It was detected at 795 cm^{-1} (Farmer, 1974). The bending band ~~is~~ appears at 540 cm^{-1} for Si–O–Al (Van Der Marel and Beutelspacher, 1976). Considering the IR analysis for illite given by Van Der Marel and Beutelspacher (1976) and Farmer (1974), it can be concluded that the studied clays are well crystallized illites.

3.1.2. Characterization of geopolymer and geopolymer/alginate adsorbents

The morphology and surface of the geopolymer and AGHB are shown in Fig. 2. Adsorbents present ~~a~~ different appearance. As expected, the AGHB showed sphericity (Fig. 2C), the beads can be seen as Ca-alginate network on the external surface layer. In the high magnification SEM image, AGHB appears to be highly porous (Fig. 2D). The beads underwent a significant reduction after consolidation at 40 °C, explained by the removal of ~~the~~ residual water. The AGHB particles sizes follow a modal distribution with the mean size centered at 87.596 μm regarding the 9.066 μm of the starting geopolymer.

The results of N_2 adsorption/desorption revealed that the BET surface area of AGHB was 9.53 m^2/g which was lower than the original geopolymer surface (13.35 m^2/g). This fact can be explained by the entry of alginate between the particles of the material. AGHB contained a large number of mesopores with an average pore size of 8.5 nm and an average pore volume of 0.020 cm^3/g, what can provide sufficient area for pollutant adsorption.

Zeta potential analysis was conducted at different pH conditions. The results (Fig. S5) reveal that zeta potential is negative for all pH values tested, what demonstrates that the surface of AGHB is negatively charged. The pH_{PZC} was practically equal to 8.4 (Fig. S6).

The XRD patterns of the foamed geopolymer and its hybrid derivative are shown in Fig. S7. The geopolymer was polymerized with the formation of semicrystalline and amorphous phases, most of the peaks have low intensities. The observed peak at 2θ around 27° is due to the semi-crystalline phase of sodium aluminum and silicate hydrate. Very low-intensity peaks of unreacted reagents can also be observed in the patterns. The XRD pattern of AGHB presents mainly amorphous structure, although still contained the peak centered at 27° as the main feature of the geopolymer.

The FTIR spectra of geopolymer and AGHB are presented in Fig. S8. Results also confirmed that AGHB was a hybrid of the geopolymer and alginate. The characteristic peaks of geopolymer could be clearly found in AGHB such as the asymmetric stretching band at 980 cm^{-1} for N-A-S-H gels (Duan et al., 2016), which overlapped the C–O–C stretching peak of alginate (Al Bakri Abdullah et al.,). The band at 876 cm^{-1} fits with the Si–O–Si asymmetric stretching mode (Shiu et al., 2014). Bands at 3360 and 1620 cm^{-1} fit with O–H stretching. The peak at 1420 cm^{-1} can be associated to a combination of the C–OH deformation vibration and carboxylate symmetric stretch vibration.

FTIR and XRD analyses were also applied after adsorption experiments with 5-FU. These results are described in mechanism study section.

3.2. Adsorption studies

3.2.1. Kinetic studies

To determine the kinetic properties, the adsorption equilibrium capacity of AGHB by 5-FU was examined at contact times from 10 min to 24 h maintaining fixed the following parameters: 2.5 mg/L for 5-FU concentration; pH of water: 7.8; 0.02 g/L for AGHB/water dosage. Fig. S9 shows the kinetic data obtained. In the first 10 min, ~50% of 5-FU was removed from the water phase. The removal continuously increased to 70% in 60 min. It can also be observed that between 1 h and 24 h no significant difference was observed ($p = 0.05$), which indicates a rapid kinetic behavior. AGHB required shorter equilibrium times than

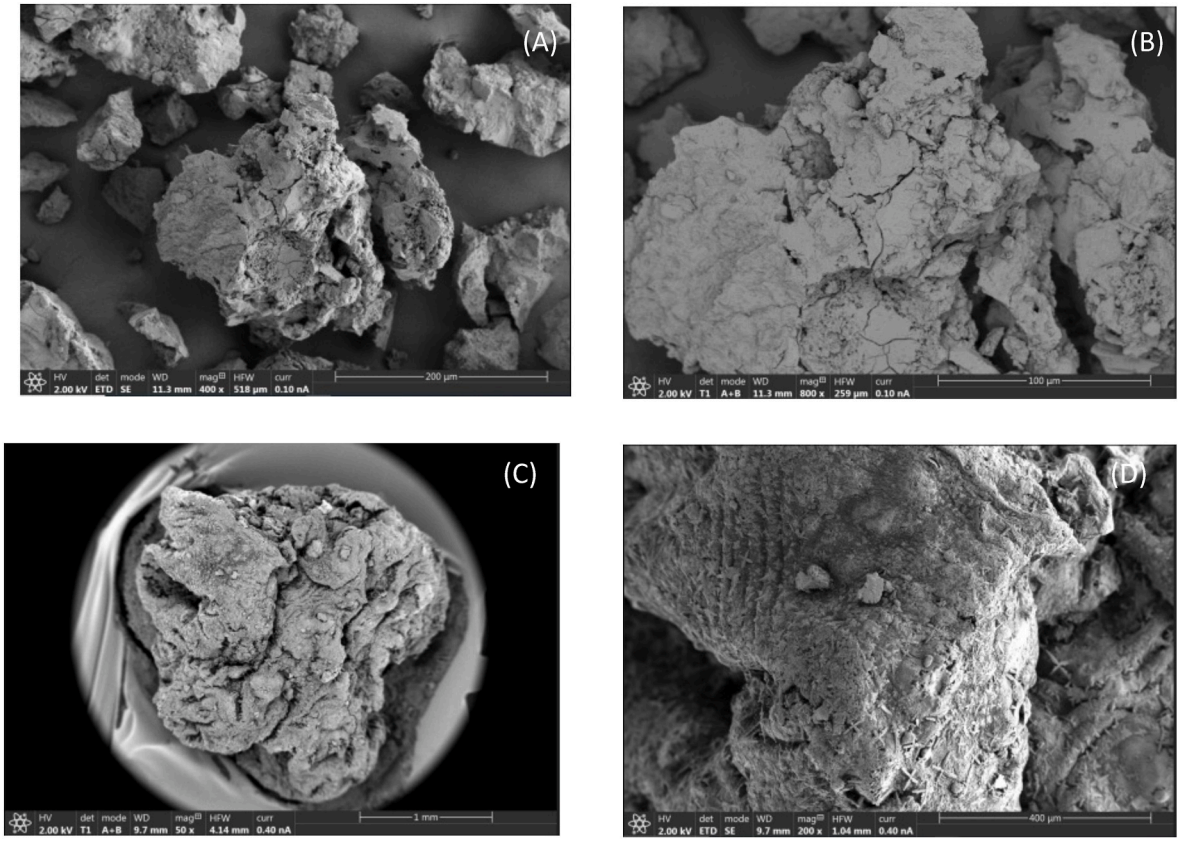

Fig. 2. SEM image of the synthetic geopolymer (A), high magnification SEM image of the synthetic geopolymer (B), SEM image of the geopolymer/alginate hybrid beads (C), and high magnification SEM image for the porous structure of the geopolymer/alginate hybrid beads (D).

other adsorbents. For example, 6 h was needed to reach a removal efficiency of 63% of 5-FU using a Zeolite HY-60 (Datt et al., 2013) whereas 26 h were required when using a thiol functionalized material (Murugan et al., 2013).

The pseudo-first-order (PFO), pseudo-second-order (PSO), and other kinetic models were applied to evaluate their goodness of fit to the experimental data. The values of the kinetic parameters, the fit correlation coefficients and the experimental error obtained from each model are presented in Table S3. The data obtained fit the PSO model better than the other models ($R^2 > 0.999$) (Fig. 3). The adsorptive removal of pollutants by geopolymers usually follows a PSO kinetic model, though pseudo-first order model has also been reported in the case of 5-FU using NiO/geopolymer (Abukhadra et al., 2022). The intraparticle diffusion model, displayed in Fig. S10, revealed two main stages in the adsorption process, a first and rapid adsorption step attributed to the diffusion of 5-FU to the exterior surface and a second and slow step ascribed to intraparticle diffusion into the pores of the adsorbent.

3.2.2. Isotherm studies

The analysis of the isotherm data by fitting them to different isotherm models such as Langmuir, Freundlich and Dubinin-Radushkevich is an important step to find the suitable model that can be used for design purposes. All the model constants and other parameters evaluated from the slopes and intercepts of the respective model equations are summarized in the supplementary material (Kheirandish et al., 2017; Pourebrahim et al., 2017; Hosseinpour et al., 2018; Jamshidi et al., 2015). In this work, isotherm models have been investigated in the concentration range of 5-FU from 0.1 to 20 mg/L. The values of the rest of variables were fixed as follows: contact time:180 min; water pH: 7.8; and AGHB/water dosage: 0.02 g/L. The adjustment parameters obtained from each model are shown in Table S4 and plotted in Fig. 3. The results showed that at the initial concentration of 5-FU (0.1 mg/L) there were enough adsorption sites on the adsorbent. That initial concentration was set at higher values than that reported in environmental waters. The increase of 5-FU concentration resulted in a lower adsorption effect due to a higher occupation of adsorption sites.

Based on fixing findings, 5-FU molecules are adsorbed onto the surface of AGHB according to the Langmuir model (R^2 0.993), involving a homogeneous distribution of active sites onto AGHB surface, since the Langmuir equation assumes that the surface is homogenous. A maximum monolayer capacity (q_{max}) of 6.28 mg/g was obtained.

The effect of temperature on the removal efficiency was also investigated using adsorption tests at different temperatures (10, 25 and 40 °C). The feasibility of the adsorption process was evaluated by thermodynamic parameters including free energy change (ΔG°), enthalpy (ΔH°), and entropy (ΔS°). ΔG° was calculated as:

$$\Delta G^\circ = -RT\ln K_d \quad (1)$$

where R is the gas constant (8.314 J/mol·K); T is the adsorption temperature (K); and K_d is the equilibrium constant (L/kg). The K_d value was calculated as q_e/C_e where q_e and C_e are the equilibrium concentrations of 5-FU on AGHB (mg/kg) and in the water solution (mg/L), respectively.

The enthalpy change (ΔH°) and entropy (ΔS°) of adsorption were estimated from the following equation:

$$\Delta G^\circ = \Delta H^\circ - T\,\Delta S^\circ \quad (2)$$

The ΔH° and ΔS° were obtained from the slope and intercept of the plot of ln K_d *versus* 1/T, respectively. The calculated thermodynamic parameters are given in Table S5. The results show that ΔG° is negative for the three temperatures evaluated, suggesting that adsorption is spontaneous. The adsorption was more favourable at lower temperatures. The amount of 5-FU adsorbed by unit weight of adsorbent decreases when temperature increases. Nevertheless, variations of the adsorption free energy with temperature were always small. The positive ΔH° value corresponds to endothermic processes, however, its magnitude is not high (9.0 kJ/mol). Since chemisorption occurs when the adsorption enthalpy change is higher than 200 kJ/mol (Kohli and Mittal, 2012), the process in this study can be classified as physical adsorption. The negative ΔS value indicates that adsorption is associated with a decrease in randomness attributed to the decrease in the freedom degree of 5-FU molecules.

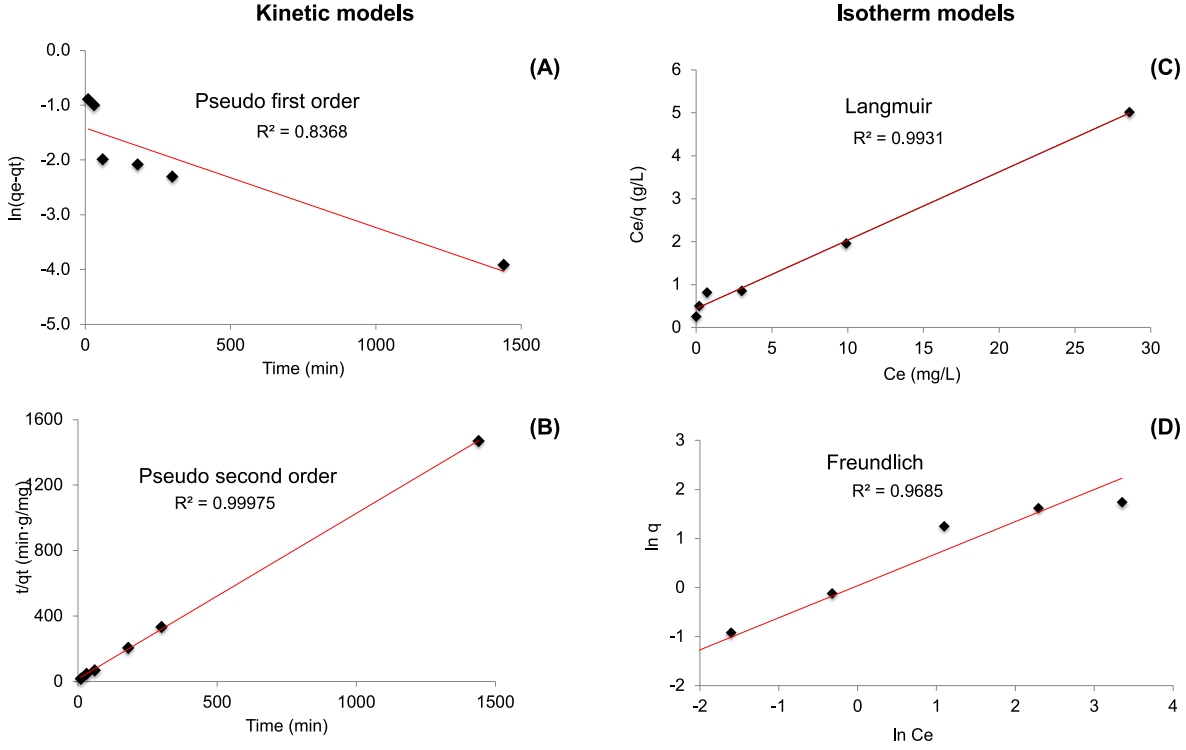

Fig. 3. Fitting with the pseudo-first-order (A), pseudo-second-order (B); and Langmuir (C), Freundlich (D) models for the adsorption of 5-FU by AGHB.

3.2.3. Influence of pH and dissolved organic matter content

The effect of pH on the adsorption of 5-FU onto AGHB was evaluated in the range from 2 to 14. The values of the other parameters were fixed at: contact time: 180 min; 5-FU concentration: 2.5 mg/L; AGHB/water dosage: 0.02 g/L. The pH was adjusted with NaOH (0.1 M) or HCl (0.1 M) solutions. The results showed that at pH 4 the adsorption percentage of 5-FU by AGHB was enhanced (Fig. 4A). This fact can be explained because 5-FU is a secondary amine with pKa = 8. A study on the pKa values indicated that neutral form dominates below pH 8 and the N1 deprotonated form dominates above pH 8. Thus, the species present in solution at pHs >8 are mainly negative charged (Wielinska et al., 2019). This phenomenon disfavors the adsorption process on negatively charged carboxyl groups immobilized onto the polymeric matrix from alginate by electrostatic repulsions. Adsorption of 5-FU promotes a variation in the surface charge from a negative value of −6.76 mV (before adsorption) to a more negative value of −9.79 mV after the adsorption assay. Furthermore, the PZC that corresponds to the surface neutrality for AGHB materials was determined at pH_{PZC} practically equal to 8.4, indicating the saturation of the AGHB surface with negative charges above this pH value. At pH = 2, the adsorption percentage decreased to <40%, what could be explained by some modification or destruction of the material structure.

The presence of DOM, commonly found in environmental samples, can represent a competition for adsorbent binding sites conditioning the adsorption process. In this work, humic acid was used in the range from 0 to 25 mg/L to represent natural DOM. It is an ordinary class of natural organic matter, with oxygen functional groups, that usually exists with a negative surface charge (Chen et al., 2018). As can be seen in Fig. 4B, the presence of DOM does not cause a significant competition on the sorption, which is favourable for applying the material in environmental waters.

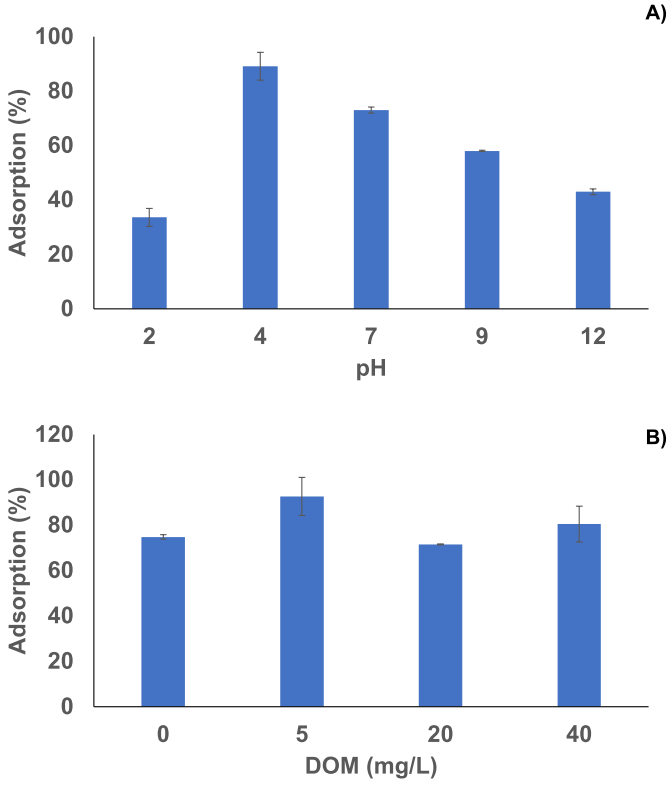

Fig. 4. Effect of pH (A) and DOM (humic acid, mg/L) (B) on the adsorption (%) of 5-FU by AGHB.

3.3. Mechanism study

According to preliminary tests, the adsorption of 5-FU was low for the geopolymer and only the modified geopolymer with sodium alginate (AGHB) adsorbed 5-FU, what is related to morphological and textural properties of the material. Different surface characteristics can be observed for AGHB before and after adsorption of 5-FU. After adsorption, the material surface become less porous (0.002 cm^3/g) and the BET surface area was reduced from 9.53 m^2/g to 1.09 m^2/g. Moreover, the average pore size of AGHB was reduced from its initial value of 9.57 mm to 6.53 nm after adsorption. These changes suggest that 5-FU was successfully loaded on AGHB surface.

The XRD patterns of AGHB after adsorption of 5-FU are described in Fig. S7. The adsorption does not affect the structure of the materials but changes the functional groups on the surface affecting the surface charges. Besides the characteristic peak of the geopolymer, a new peak at 29.4° can be observed what indicates the presence of 5-FU (Ge et al., 2019). In the IR spectrum it can be observed that, after adsorption, the small peaks of AGHB between 500 and 1500 cm^{-1} disappear, and the peak at 3200 cm^{-1} becomes wider and less intense, which can be explained by the dissolution of silicon-aluminum compounds used in the synthesis of the geopolymer (Liu et al., 2016). In addition, the height of the absorption peak of AGHB at 980 cm^{-1} increases, while the absorption peak at 1620 cm^{-1} shifts to a lower transmission direction after the adsorption of 5-FU. This fact could be explained because the functional groups of Si–O–Al can undergo coordination reactions with ions, resulting in changes in the surface charge (Kara et al., 2017).

The mechanism of pharmaceuticals adsorption by geopolymers and clay-based materials depends on the structure of the compound and the clay mineral used or surface modifications applied on the adsorbent material. Several non-covalent interactions such as hydrogen bonding, ionic, electrostatic and π–interactions have been observed and assumed to play an important role in the adsorption mechanism (Hacıosmanoglu et al., 2022; Tong et al., 2019).

The mechanism and nature of adsorption of 5-FU onto AGHB material is complex. Fig. 5 shows the proposed adsorption mechanism. 5-FU drug is a weak acid with a pKa value of 7.93 (amine). 5-FU does not exist in the protonated and double-deprotonated forms in the pH range of 0–14. The neutral form dominates below pH 8 and the N1 deprotonated form dominates above pH 8 (Wielinska et al., 2019). Therefore, at pH values higher than 7.93, it releases protons of amino groups being transformed to its anionic form. The highest adsorption on AGHB, up to 80%, occurred at pH 4.0 at which 5-FU is in its neutral form. Consequently, it can be deduced that 5-FU adsorption does not take place through electrostatic interactions. On the other hand, besides pore filling, the hydroxyl and carboxyl groups from alginate immobilized into the polymeric matrix provides sites for strong dipole interactions between hydrogen-acceptor atoms such as N, O, or F present in 5-FU molecules. Further, a n-π interaction can be created between the aromatic structure of the 5-FU bonds and hydroxyl groups of alginate or the Si–O–Si bonds in the structure of the porous geopolymer. Similarly, Abukhadra et al. (2022) explained the 5-FU adsorption mechanism NiO/geopolymer nanocomposite by physical mechanisms including the hydrogen bonding, van der Waals forces, and dipole bonding forces. In another attempt, Datt et al. (2013) suggested that zeolite HY-5 has the capacity to interact with the 5-FU species both by hydrogen bonding as well as coordination complexation.

The IR spectrum after adsorption indicated that the observed changes were not intense. This fact could be probably due to the weak interactions in the adsorption mechanism and because the adsorption mechanism involved physical interactions in the surface adsorption rather than chemical bondings. This behavior is desirable for reusability of the adsorbent.

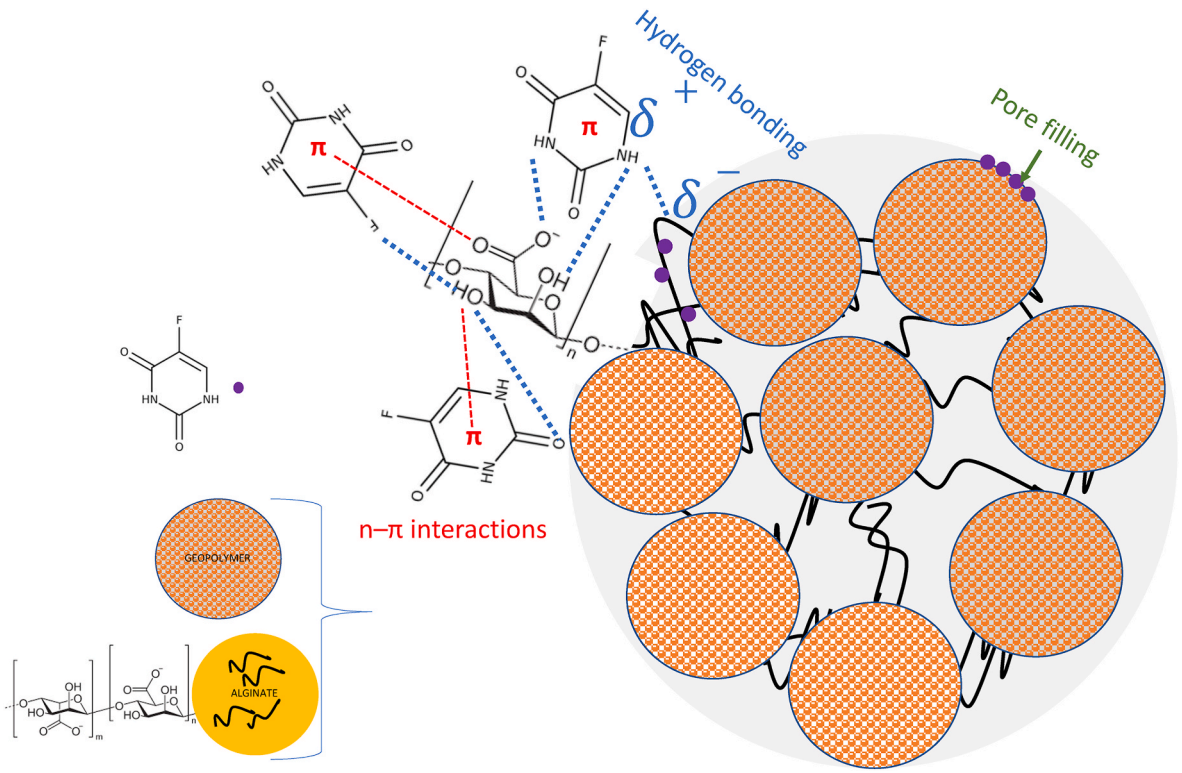

Fig. 5. Possible mechanism for 5-FU ions adsorption on AGHB composite.

3.4. Desorption and reuse

Reusability of an adsorbent is important to be assessed for its long-term applicability. For this purpose, four adsorption-desorption cycles were applied for AGHB and the changes in the amounts of 5-FU adsorbed per unit weight of the adsorbent were calculated. Results reveals that the reuse potential of AGHB is very high, i.e., the percent adsorption capacities retained after four reuse cycles were 89.9, 93.5, 75.5, 24.1% for 5-FU. This fact can be also explained by the weak surface adsorption. The reusability of the material is compromised after the fourth reuse cycle. This decrease is often observed in similar materials. For example, Maged et al. (2020) reported that the adsorption efficacy of tetracycline on activated bentonite clay was reduced to 30% after five cycles. Other authors have studied reusability in materials for which the decrease in adsorption efficacy is observed already in the third cycle. For example, Chauhan et al. (2020) concluded that their clay intercalated with Zr pillars could only be reused three times for the adsorption of drugs and personal care products, as in the third cycle the adsorption efficiency was considerably reduced. Therefore, the possibility of carrying out three absorption cycles is a reasonable compromise between the reusability of the material and the efficiency of the absorption.

Very small adsorbent particles can float on wastewater making them difficult to recycle. In addition, the pressure generated in the wastewater treatment column is much higher than when bigger adsorbent particles are used. Millimetric particles are simple to post-process and the pressure passed through the column is much smaller, and hence, are regarded as one of the most widespread adsorbents employed in the column for dynamic removal of pollutants (Luhar and Luhar, 2021).

3.5. Adsorption in environmental real matrices

Finally, to achieve greater environmental realism, the adsorption test were repeated using fortified (2.5 mg/L of 5-FU) influent and effluent wastewater and surface water. Contact time was fixed at 180 min and AGHB/water dosage at 0.02 g/L. Surface water was collected from the Guadalquivir River (Seville, Spain). Influent and effluent wastewater were sampled from a wastewater treatment plant located in Seville (Spain). Before the experiments, the samples were filtered through a 1.2 μm glass-microfiber membrane filter. The quantification was carried out in each case using matrix-matched calibration curves to avoid matrix effect. The adsorption capacity in environmental water matrices was approximately 80% which is an extremely high value considering the complexity of the matrix (Fig. S11). The adsorption capacities of 5-FU for water remediation using geopolymer or other biopolymer-based materials are limited, as can be seen in Table 1. Materials involving clays (Golubeva et al., 2020), zeolites (Gomar and Yeganegi, 2017; Spanakis et al., 2014; Datt et al., 2013), modified carbon nanotubes (Yahyavi et al., 2020), carbon nitride (Zaboli et al., 2020) and mesoporous silica (Benová et al., 2020; Azali et al., 2019) have also been studied for drug delivery but not for water remediation. Nevertheless, in spite of the useful properties of the above-mentioned materials, their cost is still a limitation for their wide application in water purification treatments where the use of adsorbents based on natural precursors is recommended. A direct comparison of AGHB with other adsorbents is quite complicated due to the different experimental conditions used. Nevertheless, the adsorption efficiency achieved by the synthetized AGHD on the removal of 5-FU is among the highest results (>80%). Recently, Abukhadra et al. (2022) developed an effective NiO/geopolymer for the removal of 5-FU, although it was not tested with real samples. It is difficult to make a direct comparison with other adsorbents since the concentration range tested in most of the studies were much higher (usually about 1000 mg/L, reaching values up to 12,000 mg/L (Datt et al. (2013)) than in our study (0.1–40 mg/L). This fact can be explained because those works were focused on other applications such as drug release. In this study lower concentrations tested were in concordance to the levels reported for this contaminant in environmental samples (Lin and Lin, 2014). Abukhadra et al. (2022) applied lower 5-FU concentrations (50–350 mg/L) than other authors in a decontamination study. Nevertheless, such concentrations were still higher than those employed in this study.

Table 1
Comparison between the adsorption capacity of AGHB and other assessed materials in literature.

Adsorbent		Adsorption efficacy (%)	Concentration range tested (mg/L)	Q_{max} (mg/g)	Application	Reference
Clay	Montmorillonite-Magnetite	7.43	250–4000	59.44	Loading	Çiftçi et al. (2020)
	Montmorillonite-Magnetite-N_2	6.05		48.38		
	Modified montmorillonite	44% after 30 min	–	–	Encapsulation	Gârea et al., 2015
Modified carbon nanotubes	Molecular imprinted MWCNT	–	1.6×10^{-7} - 2.2×10^{-7}	0.65	Artificial receptors	Mathew and Abraham (2014)
Silica	Mesoporous silica nanoparticles	95.27% after 24 h	20–100		Loading	Azali et al. (2019)
	Mesoporous silica SBA-15		100–6500	92.63	Loading	Benová et al. (2020)
	Mesoporous silica SBA-15_N-ANI			55.3		
	Magadiite	39.3% after 6 h	1000	98.18	Drug carrier	Ge et al. (2019)
	Magadiite-CTAB	52.2% after 6 h		130.59		
	Magadiite-CTAB-CS	64.9% after 6 h		162.29		
	MCM-41	86% after 12 h	1000		Encapsulation	Murugan et al. (2013)
	Thiol-functionalized MCM-41	99% after 12 h				
Zeolite	Zeolite HY-5		1.2×10^{4}	110	Loading	Datt et al. (2013)
	Zeolite HY-30			105		
	Zeolite HY-60			90		
	Zeolite BEA	6.02% after 24 h	2.66×10^{3}	24.08	Encapsulation	Spanakis et al. (2014)
	Zeolite NaX-FAU	16.18% after 24 h		64.72		
	Zeolite ZIFs			650–680	Drug carrier	Gomar and Yeganegi, 2017
Geopolymers	NiO/Geopolymer	99%, 300 min	50–350	329.7	Decontamination	Abukhadra et al. (2022)
	AGHB	>80% after 3 h	0.1–40		Decontamination	This work

3. Conclusion

This study shows the potential of a new and low-cost adsorbent synthetized through extrusion method based on alginate and a geopolymer (prepared from an illito-kaolinitic clay) for the decontamination of 5-FU from water resources. In addition to be a low-cost and eco-friendly material, the use of this sorbent presents other advantages such as AGHB exhibited a rapid and excellent adsorption capacity for 5-FU, explained by its porous structure and the cooperative effect of sodium alginate through hydrogen bonds. The adsorption of 5-FU occurred according to PSO kinetic and Langmuir isotherm as classic models. The percentage of adsorption was significantly affected by the pH values, decreasing when the negative ionic fraction of 5-FU increased and at pH > pHpzc.

The main advantages of the prepared AGHB and the present study can be summarized as follows:

- A new formulation focused on the preparation of cross-linked adsorbent beads of alginate/geopolymer has been carried out.
- The geopolymer synthesized in this work has a distinct formulation, since materials created by combining illito-kaolinitic clay, silica fume and sodium hydroxide have not been previously reported in the literature.
- The use of waste glass by-product from other industries.
- AGHB is a low-cost and eco-friendly material, that exhibited a rapid and excellent adsorption capacity for 5-FU.
- Using millimetric particle material makes the beads easy to handle and resistant to the recovery, separation, and filtration operations of aqueous systems.
- The high adsorption capacity of AGHB for 5-FU in wastewater and superficial water samples supports its applicability for the purification of contaminated water.

Nevertheless, there are also limitations:

- Laboratory experiments using packed column mode tests need to be conducted to evaluate the continuous removal behavior of 5-FU by AGHB and to predict the breakthrough performance.
- The millimetric particles are simple to post-process. However, the pressure passed through the column is much smaller, and hence, it may diminish the adsorption competence.
- The evaluation of the interaction with multicomponent in column and batch processes and application to a broad range of analytes are required.
- The performance of porous geopolymers still needs to be improved at large-scale fabrication level and with a study of estimated costs.

Credits authors

Conceptualization, A.B.A., J.M., O.A., E.A.; methodology, A.B.A., J. M., J.L.S., M.A.; investigation, A.B.A., J.M., M.A.; resources, A.B.A., O. A., M.A.; writing—original draft preparation, A.B.A., J.M.; writing—review and editing, J.M., J.L.S.; visualization, O.A., N·H., J.L.S., I. A.; supervision, E.A.; project administration, E.A. and I.A.; funding acquisition, O.A., E.A., I.A. and J.L.S. All authors have read and agreed to the published version of the manuscript.

Declaration of competing interest

The authors declare that they have no known competing financial interests or personal relationships that could have appeared to influence the work reported in this paper.

Data availability

Data will be made available on request.

Acknowledgment

This work was financially supported by the Ministerio de Ciencia e Innovación from the Spanish Government (Project No. PID2020-117641RB-I00) and by the Junta de Andalucía (Consejería de Economía y Conocimiento, Project I + D + i PAIDI Andalucía No. P20_00556). Ben AMOR received a fellowship for an internship from Ministry of Higher Education and Scientific Research of Republic of Tunisia.

Appendix A. Supplementary data

Supplementary data to this article can be found online at https://doi.org/10.1016/j.chemosphere.2023.139092.

References

Abukhadra, M.R., AlHammadi, A.A., Khim, J.S., Ajarem, J.S., Allam, A.A., Shaban, M.S., 2022. Enhanced adsorption and visible light photocatalytic removal of 5-Fluorouracil residuals using environmental NiO/geopolymer nanocomposite: steric, energetic, and oxidation studies. J. Environ. Chem. Eng. 10, 108569.

Aichour, A., Zaghouane-Boudiaf, H., 2020. Synthesis and characterization of hybrid activated bentonite/alginate composite to improve its effective elimination of dyes stuff from wastewater. Appl. Water Sci. 2020, 10–146. https://doi.org/10.1007/s13201-020-01232-0.

Al Bakri Abdullah, M.M., Hussin, K., Bnhussain, M., Ismail, K.N., Yahya, Z., Razak, R.A., Fly ash-based geopolymer lightweight concrete using foaming agent. Int. J. Mol. Sci. 13, 7186-7198.

Al-husseiny, R.A., Ebrahim, S.E., 2021. Synthesis of geopolymer for the removal of hazardous waste: a review. IOP Conf. Ser. Earth Environ. Sci. 779, 012102 https://doi.org/10.1088/1755-1315/779/1/012102.

Azali, N.S., Kamarudin, N.H.N., Rahim, A.R.A., Nasir, N.S.J., Timmiati, S.N., Jaafar, N.F., 2019. Adsorption and release of 5-fluorouracil (5FU) from mesoporous silica nanoparticles. Mater. Today: Proc. 19, 1722–1729.

Benová, E., Bergé-Lefranc, D., Zelenák, V., Almási, M., Huntosová, V., Hornebecq, V., 2020. Adsorption properties, the pH-sensitive release of 5-fluorouracil and cytotoxicity studies of mesoporous silica drug delivery matrix. Appl. Surf. Sci. 504, 144028.

Booker, V., Halsall, C., Llewellyn, N., Johnson, A., Williams, R., 2014. Prioritising anticancer drugs for environmental monitoring and risk assessment purposes. Sci. Total Environ. 473, 159–170. https://doi.org/10.1016/j.scitotenv.2013.11. 145. –474.

Caillère, S., Hénin, S., Rautureau, M., 1982. Minéralogie Des Argiles. I. Structure et propriétés physico-chimiques. Masson, Paris, p. 184.

Chauhan, M., Saini, V.K., Suthar, S., 2020. Enhancement in selective adsorption and removal efficiency of natural clay by intercalation of Zr-pillars into its layered nanostructure. J. Clean. Prod. 258, 120686 https://doi.org/10.1016/j.jclepro.2020.120686.

Chen, W., Ouyang, Z., Qian, C., Yu, H., 2018. Induced structural changes of humic acid by exposure of polystyrene microplastics: a spectroscopic insight. Environ. Pollut. 233, 269–7491. https://doi.org/10.1016/j.envpol.2017.10.027.

Çiftçi, H., Arpa, M.D., Gülaçar, I.M., Ozcan, L., Ersoy, B., 2020. Development and evaluation of mesoporous montmorillonite/magnetite nanocomposites loaded with 5-Fluorouracil. J. Micropor. Mesopor. Mater. 303, 110253.

Datt, A., Burns, E.A., Dhuna, N.A., Larsen, S.C., 2013. Loading and release of 5-fluorouracil from HY zeolites with varying SiO2/Al2O3 ratios. Microporous Mesoporous Mater. 167, 182–187.

Davidovits, J., 2008. Geopolymers Chemistry and Applications. Saint-Quentin, France, Institut Geopolymere.

de Oliveira Klein, M., Serrano, S.V., Santos-Neto, A., da Cruz, C., Brunetti, I.A., Lebre, D., Gimenez, M.P., Reis, R.M., Silveira, H.C.S., 2021. Detection of anti-cancer drugs and metabolites in the effluents from a large Brazilian cancer hospital and an evaluation of ecotoxicology. Environ. Pollut. 268, 115857.

Dinesh, G.K., Chakma, S., 2019. Mechanistic investigation in degradation mechanism of 5-Fluorouracil using graphitic carbon nitride. Ultrason. Sonochem. 50, 311–321. https://doi.org/10.1016/j.ultsonch.2018.09.032.

Duan, P., Yan, C., Zhou, W., Luo, W., 2016. Fresh properties, mechanical strength and microstructure of fly ash geopolymer paste reinforced with sawdust. Construct. Build. Mater. 111, 600–610.

Farmer, V.C., 1974. The layers silicates. The Infrared Spectra of Minerals Monograph 4, 331–363. Mineralogical Society, London.

Gârea, S.A., Mihai, A.I., Ghebaur, A., Nistor, C., Sârbu, A., 2015. Porous clay heterostructures: a new inorganic host for 5-fluorouracil 2 encapsulation. Int. J. Pharm. 491, 299–309.

Ge, M., Tang, W., Du, M., Liang, G., Hu, G., Alam, S.J., 2019. Research on 5-fluorouracil as a drug carrier materials with its in vitro release properties on organic modified magadiite. Eur. J. Pharmaceut. Sci. 130, 44–53.

Ge, Y., Cui, X., Liao, C., Li, Z., 2017. Facile fabrication of green geopolymer/alginate hybrid spheres for efficient removal of Cu(II) in water: batch and column studies. Chem. Eng. J. 311, 126–134.

Golubeva, O.Y., Alikina, Y.A., Brazovskaya, E.Y., Ugolkov, V.V., 2020. Peculiarities of the 5- fluorouracil adsorption on porous aluminosilicates with different morphologies. Appl. Clay Sci. 184, 105401.

Gomar, M., Yeganegi, S., 2017. Adsorption of 5-fluorouracil, hydroxyurea and mercaptopurine drugs on zeolitic imidazolate frameworks (ZIF-7, ZIF-8 and ZIF-9). Microporous Mesoporous Mater. 252, 167–172.

Hacıosmanoglu, G.G., Mejías, C., Martín, J., Santos, J.L., Aparicio, I., Alonso, E., 2022. Antibiotic adsorption by natural and modi ed clay minerals as designer adsorbents for wastewater treatment: a comprehensive review. J. Environ. Manag. 317, 115397.

Heath, E., Isidori, M., Kosjek, T., Filipic, M. (Eds.), 2020. Fate and Effects of Anticancer Drugs in the Environment. © Springer Nature Switzerland AG.

Hosseinpour, S.A., Karimipour, G., Ghaedi, M., Dashtian, K., 2018. Use of metal composite MOF-5-Ag2O-NPs as an adsorbent for the removal of Auramine O dye under ultrasound energy conditions. Appl. Organomet. Chem. 32, e4007.

Jamshidi, M., Ghaedi, M., Dashtian, K., Bazrafshan, S.H.A., 2015. Ultrasound-assisted removal of Al3+ ions and Alizarin red S by activated carbon engrafted with Ag nanoparticles: central composite design and genetic algorithm optimization. RSC Adv. 5, 59522.

Kara, I., Yilmazer, D., Akar, S.T., 2017. Metakaolin based geopolymer as an effective adsorbent for adsorption of zinc(II) and nickel(II) ions from aqueous solutions. Appl. Clay Sci. 139, 54–63.

Kheirandish, S., Ghaedi, M., Dashtian, K., Heidari, F., Pourebrahim, F., Wang, S., 2017. Chitosan extraction from lobster shells and its grafted with functionalized MWCNT for simultaneous removal of Pb2+ ions and eriochrome cyanine R dye after their complexation. Int. J. Biol. Macromol. 102, 181–191.

Kohli, R., Mittal, K.L., 2012. Developments in Surface Contamination and Cleaning: Detection, Characterization, and Analysis of Contaminants. William Andrew Publishing. https://doi.org/10.1016/B978-1-4377-7883-0.10001-X. ISBN 9781437778830.

Kosjek, T., Perko, S., Zigon, D., Heath, E., 2013. Fluorouracil in the environment: analysis, occurrence, degradation and transformation. J. Chromatogr. A 1290, 62–72.

Kulaksız, E., Kayan, B., Gözmen, B., Kalderis, D., Oturan, N., Oturan, M.A., 2022. Comparative degradation of 5-fluorouracil in aqueous solution by using H2O2-modified subcritical water, photocatalytic oxidation and electro-Fenton processes. Environ. Res. 204, 111898.

Li, Z., Ge, Y., Wan, L., 2015. Fabrication of a green porous lignin-based sphere for the removal of lead ions from aqueous media. J. Hazard Mater. 285, 77–83.

Lin, H.H.-H., Lin, A.Y.-C., 2014. Photocatalytic oxidation of 5-fluorouracil and cyclophosphamide via UV/TiO2 in an aqueous environment. Water Res. 48, 559–568.

Liu, Y., Yan, C., Zhang, Z., Wang, H., Zhou, W., 2016. A comparative study on fly ash, geopolymer and faujasite block for Pb removal from aqueous solution. Fuel 185, 181–189.

Luhar, I., Luhar, S., 2021. Rubberized geopolymer composites: value-added applications. J. Compos. Sci. 5, 312.

Maged, A., Iqbal, J., Kharbish, S., Ismael, I.S., Bhatnagar, A., 2020. Tuning tetracycline removal from aqueous solution onto activated 2:1 layered clay mineral: characterization, sorption and mechanistic studies. J. Hazard Mater. 384 https://doi.org/10.1016/j.jhazmat.2019.121320.

Martín, J., Orta, M.M., Medina-Carrasco, S., Santos, J.L., Aparicio, I., Alonso, E., 2019. Evaluation of a modified mica and montmorillonite for the adsorption of ibuprofen from aqueous media. Appl. Clay Sci. 171, 29–37.

Mathew, B., Abraham, J., 2014. Synthesis and characterization of molecular imprinted polymer on multiwalled carbon nanotube for the recognition of 5-fluorouracil. Int. J. Chem. Sci. 12 (2), 695–707.

Medri, V., Papa, E., Lizion, J., Landi, E., 2020. Metakaolin-based geopolymer beads: production methods and characterization. J. Clean. Prod. 244, 118844 https://doi.org/10.1016/j.jclepro.2019.118844.

Misík, M., Filipic, M., Nersesyan, A., Kundi, M., Isidori, M., Knasmueller, S., 2019. Environmental risk assessment of widely used anticancer drugs (5-fluorouracil, cisplatin, etoposide, imatinib mesylate). Water Res. 164, 114953.

Murugan, B., Ramana, L.N., Gandhi, S., Sethuraman, S., Krishnan, U.M., 2013. Engineered chemoswitchable mesoporous silica for tumor-specific cytotoxicity. J. Math. Chem. B 28, 3494–3505.

Orias, F., Perrodin, Y., 2014. Pharmaceuticals in hospital wastewater: their ecotoxicity and contribu- tion to the environmental hazard of the effluent. Chemosphere 115, 31–39. https://doi.org/10.1016/j.chemosphere.2014.01.016.

Orta, M.M., Martín, J., Medina-Carrasco, S., Santos, J.L., Aparicio, I., Alonso, E., 2020. Biopolymer-clay nanocomposites as novel and ecofriendly adsorbents for environmental remediation. Appl. Clay Sci. 198, 105838.

Papa, E., Natali Murri, A., Vaccari, A., Landi, E., Medri, V., 2021. Geopolymer-hydrotalcite hybrid beads by ionotropic gelation. Appl. Clay Sci. 215, 106326.

Pourebrahim, F., Ghaedi, M., Dashtian, K., Heidari, F., Kheirandish, S., 2017. Simultaneous removing of Pb2+ ions and alizarin red S dye after their complexation by ultrasonic waves coupled adsorption process: spectrophotometry detection and optimization study. Ultrason. Sonochem. 35, 51–60.

Shiu, H.-S., Lin, K.-L., Chao, S.-J., Hwang, C.-L., Cheng, T.-W., 2014. Effects of foam agent on characteristics of thin-film transistor liquid crystal display waste glass-metakaolin-based cellular geopolymer. Environ. Prog. Sustain. Energy 33, 538–550.

Spanakis, M., Bouropoulos, N., Theodoropoulos, D., Sygellou, L., Ewart, S., Moschovi, A. M., Siokou, A., Niopas, I., Kachrimanis, K., Nikolakis, V., Cox, P.A., Vizirianakis, I.S., Fatouros, D.G., 2014. Controlled release of 5-fluorouracil from microporous zeolites. Nanomedicine 10 (1), 197–205. https://doi.org/10.1016/j.nano.2013.06.016.

Tong, Y., McNamara, P.J., Mayer, B.K., 2019. Adsorption of organic micropollutants onto biochar: a review of relevant kinetics, mechanisms and equilibrium. Environ. Sci. Water Res. Technol. 5, 821–838.

Ucankus, G., Ercan, M., Uzunoglu, D., Culha, M., 2018. Methods for preparation of nanocomposites in environmental remediation. New Polim. Nanocompos. Environ. Rem. 1, 1–28.

Van Der Marel, H.W., Beutelspacher, H., 1976. Atlas of Infrared Spectroscopy of Clay Minerals and Their Ad-Mixtures. Elsevier, Amsterdam, pp. 31–58.

Wielinska, J., Nowacki, A., Liberek, B., 2019. 5-Fluorouracil—complete insight into its neutral and ionised forms. Molecules 24, 3683. https://doi.org/10.3390/molecules24203683, 2019.

Wilczewska, P., Pancielejko, A., Luczak, J., Kroczewska, M., Lisowski, W., Siedlecka, E. M., 2022. The influence of ILs on TiO2 microbeads activity towards 5-FU removal under artificial sunlight irradiation. Appl. Surf. Sci. 573, 151431.

Yahyavi, M., Badalkhani-Khamseh, F., Hadipour, N.L., 2020. Adsorption behavior of pristine, Al-, and Si-doped carbon nanotubes upon 5-fluorouracil. Chem. Phys. Lett. 750, 137492.
Zaboli, A., Raissi, H., Farzad, F., Hashemzadeh, H., 2020. Assessment of adsorption behavior of 5-fluorouracil and pyrazinamide on carbon nitride and folic acid-conjugated carbon nitride nanosheets for targeting drug delivery. J. Mol. Liq. 301, 112435.
Zhang, Y., Xiao, Y., Zhang, J., Chang, V.W.C., Lim, T.T., 2017. Degradation of cyclophosphamide and 5-fluorouracil in water using UV and UV/H2O2: kinetics investigation, pathways and energetic analysis. J. Environ. Chem. Eng. 5, 1133–1139. https://doi.org/10.1016/j.jece.2017.01.013.